"FLUID DYNAMICS APPLICATIONS IN GROUND TRANSPORTATION: Simulation, a primary delepment tool in the automotive industry", Lyon, France, 2005

# Time-Dependent Simulations for the Directional Stability of High Speed Trains Under the Influence of Cross Winds or Cruising Inside Tunnels

Siniša Krajnović*and Hassan Hemida
Division of Fluid Dynamics,
Department of Applied Mechanics,
Chalmers University of Technology, SE-412 96 Göteborg, Sweden

Ben Diedrichs
Division of Railway Technology,
Department of Aeronautical and Vehicle Engineering
Royal Institute of Technology, SE-100 44 Stockholm, Sweden

## Abstract

Large eddy simulation (LES) technique is used to study safety and comfort issues of cross-wind stability and lateral vehicle vibrations in double-track tunnels. A simplified train model is used to study flows at yaw angles of $90^o$ and $35^o$ of the cross wind and Reynolds numbers of $3 \times 10^5$ and $3.7 \times 10^5$, respectively. LES results are compared with the experimental data and good agreement was found. For the LES investigation of lateral vibrations in tunnel, two high-speed trains are used, the German ICE2 and the Japanese Shinkansen S300. It is found that the lateral oscillations of the Shinkansen train originate from the shape of the rear end. Besides, the small vortices formed at the front of the train, on the center side of the tunnel, are found to govern the separation at the rear of the Shinkansen train. The frequency of the lateral oscillations of the Shinkansen train in LES is $St = 0.09$ compared to $St = 0.1$ measured at full scale tests. In the same time no dominant frequency is found on the ICE2 train.

## 1 Introduction

Increasing the speed and decreasing the weight of high-speed trains have lead to increased sensitivity to cross-wind effects. Also in the situations without cross winds, the aerodynamics can influence the train in the lateral direction. This happens when the train is moving inside narrow double-track tunnels. These and similar aerodynamic phenomena are difficult to study in a wind tunnel due to difficulties to simulate the windy conditions. Although specifying such a boundary condition in a numerical simulations is fairly simple, results of numerical simulations are dependent on the numerical method used. Three numerical approaches dominate in simulation of turbulent flows: direct numerical simulation (DNS), Reynolds-Averaged Navier-Stokes (RANS) equations simulation and large eddy simulation (LES). In the following section we briefly describe these methods and thereby motivate the choice of LES for flows around high-speed trains in this work. This is followed by the description of LES of two different flows and their results.

*Tel: (+46)31-772 5272, E-mail: sinisa@chalmers.se

## 2 Numerical method

The purpose of this section is not to give an extensive description of existing numerical techniques. Its only aim is to illustrate their differences and motivate the use of large eddy simulation technique in the present work.

The most straightforward approach of simulating turbulent flows is solving time-dependent Navier-Stokes equations resolving all turbulent scales. This method is called direct numerical simulation (DNS). Unfortunately, turbulent scales become smaller as the Reynolds number is increased implying that only relatively simple flows at low Reynolds number can be simulated with todays computer resources. Although computer power is improving for every year the simulation of flow around high-speed train with this technique will not be possible in next 50 years.

An alternative approach is to solve only time-averaged, so called Reynolds-Averaged Navier-Stokes equations. As a result of this averaging a new term, so called Reynolds stress, appears in the equations representing the turbulence. This term must be modeled in order to solve the equations. During the last 30 years large number of turbulent models were developed and many of them have proved to be successful in a large number of turbulent flows. However there are regions in turbulent flows where turbulence cannot be modeled accuaretely with the existing models. One such region is recirculating flow in the wake behind a train or in the case of cross wind on the side of the train. There are two chief reasons for this inability of RANS simulations to deal with such flows; flow in the wake contain wide spectrum of turbulence length and time scales while turbulence models contain often only one time and length scale; flow has inherently unsteady character. Beside their deficiency to deal with wake flows, RANS simulations dominate in industrial applications due to their relatively low computational cost.

An intermediate technique between DNS and RANS is large eddy simulation (LES). In LES filtered time-dependent Navier-Stokes equations are solved. This *filtering* is spatial and often implies averaging over computational cells. As a result of filtering only turbulent structures that are larger than computational cells are resolved (computed). Similar to the Reynolds stresses resulting from the time averaging in RANS equations, a new term describing the influence of the unresolved structures to the resolved ones appear as a result of filtering (volume averaging). This term in the equation is called sub-grid scale Reynolds stress and must be modeled. Although there is a modeling of turbulence in both RANS and LES, there is a big difference. In a RANS simulation all the turbulence is modeled and all instantaneous information is lost. A LES simulation computes most of the turbulence and only the influence of small part of turbulence (normally less than 20%) is modelled. Computational cost of a LES of wall bounded flow is much higher than that of a RANS simulations. Near wall region contain so called low- and high-speed streaks which are responsible for most of the turbulent kinetic energy production in that region. Unfortunatelly the physical extension of these structures decreases with increased Reynolds number and their typical thicknes is around 20 wall units (wall units are physical lengths normalised by the friction velocity $u_\tau$ and the kinematic viscosity $\nu$, i.e., $x^+ = xu_\tau/\nu$, $y^+ = yu_\tau/\nu$ and $z^+ = zu_\tau/\nu$). This implies that their resolution for a flow around high-speed train at operating conditions is infeasible with existing computer resources. Thus LES cannot be used for prediction of the aerodynamic forces at real trains. The proper use of LES is that of flows around model trains at lower Reynolds number. If the flow mechanisms at lower Reynolds numbers are similar to those at real-scale conditions than the obtained knowledge from LES can be used to understand the flow around real-scale train and help to optimize its design. Similar approach is already used for the flows around road vehicles [6, 7, 8, 9]. In the following sections we shall demonstrate use of this approach for studing of two stability problems of high-speed trains.

## 3 Cross wind stability

In this section we present our simulations of the flow around train model in a cross wind. For our study we have used a simplified model of the train by Chiu and Squires [1] shown in Fig. 1. The profile of the cross section of this model is defined by the following equation

$$|y|^n + |z|^n = c^n \quad (1)$$

$c = 62.5$mm ($D/2$) and $n = 5$ gives a diameter of 125mm. The cross section of the front of the train is also given by the Eq. 1 but here $c$ varies according to a semi-elliptical profile with a major diameter of $1.28D$ and $n$ decreases uniformly to 2 at the tip of the front (see Fig. 1). The total length of the train is $10D$. The cross section of the tunnel and the ground clearance of $0.15D$ are the same as in the experimental setup [1]. The distances from the model to the inlet and the outlet are $8D$ and $21D$, respectively. Similar distances are used in our previous work [6, 7, 8, 9] and these are chosen to avoid interference of the boundaries with the flow around the train model.

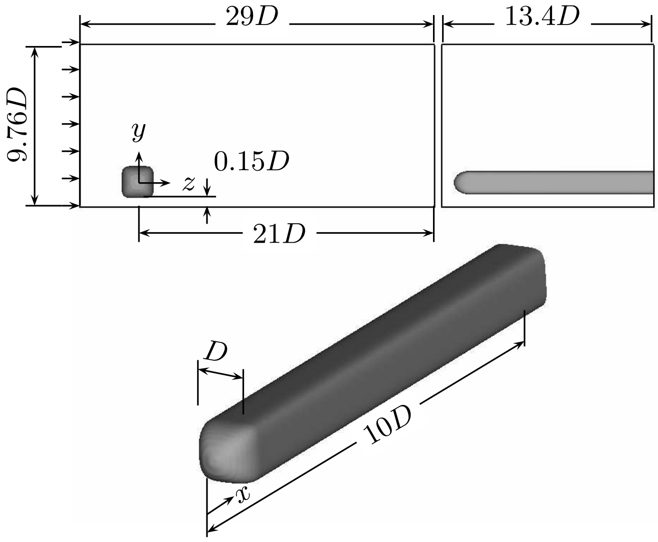


Figure 1: Computational domain and the train model influenced to the cross wind at an yaw angle of $90^o$. Upper left figure: view from the side. Upper right figure: view from the inlet.

Flow at two yaw angles of cross wind of $90^o$ and $35^o$ are simulated in our LES. Reynolds numbers of flows are $3 \times 10^5$ and $3.7 \times 10^5$ for the $90^o$ and $35^o$ yaw angles, respectively, based on the inlet velocity and the height of the train, $D$. Experimental data for both these angles are obtained in [1].

## 3.1 Boundary conditions and numerical method

In agreement with the experiments, solid walls were simulated on the floor, roof and the lateral walls of the channel. No-slip boundary conditions were used on the surface of the train and the floor, while the instantaneous wall functions [6] were applied on the lateral walls and the ceiling of the channel. Wall functions are not expected to give an accurate predictions of the near-wall flow but should be sufficient to predict the approximate boundary layer thickness and thereby the blockage ratio in the channel cross section. Convective outlet boundary condition $\partial \bar{u}_i/\partial t + U_\infty(\partial \bar{u}_i/\partial z) = 0$ is used at the outlet. Such an outlet boundary condition is prefered compared to the homogeneous Neumann condition as it decreases the influence of the outlet on the upstream flow (especially wake flow).

Two computational grids of different size are used for the simulations. These contain 8 and 11.5 million cells for the $90^o$ yaw angle case and 8 and 16 million cells for the $35^o$ yaw angle case. Using clever block topology with several $O$ and $U$ grids we were able to obtain good resolution of the near wall structures. For example, the near wall resolution in the $90^o$ yaw angle case using fine grid expressed in the wall units is 1.5 in the wall-normal direction, around 125 in the streamwise direction and around 50 in the direction parallel with the surface of the body and orthogonal to the streamwise and the wall-normal directions. Details about computational grids and numerical details can be found in [5].

### 3.2 Results

Our first simulations were that of the $90^o$ yaw angle. Results obtained from our LES are compared with the existing experimental data. We have found that the agreement of the surface pressure coefficient from LES with that from the experiment was good in all parts of the flow (see Fig. 2). Some differences are visible on the top and the bottom surfaces of the train model. These can be explained by the presence of the trip wire in the experimental study and their absence in our LES. The exact positions of the trip wires are not reported and it is not clear how to model these in a LES. Thus these were not included or modeled in our LES. Such a difference in the boundary conditions on the train model resulted in attached and weakly separated flow in the experiment and our LES, respectively. Another issue is the resolution in the direction of the train. Resolution in this direction of 50 wall units is not sufficient to resolve the near-wall streaks. However there is not much space from the front to the rear face of the train ($D$) for boundary layer to develop and the influence of these structures is probably not large.

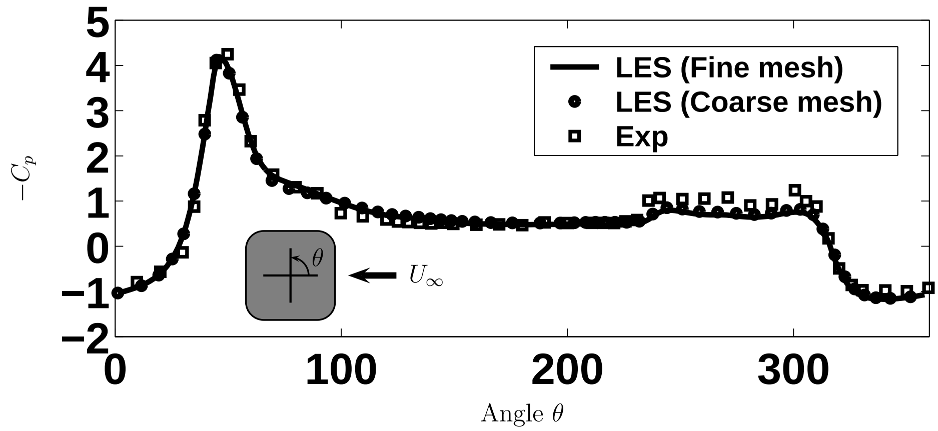


Figure 2: $90^o$ yaw angle. Time-averaged local surface pressure coefficient $C_p$ at $x/D =$ 6.5.

Comparison of the surface flow patterns from our LES with those from the experiment are shown in Fig. 3. As can be seen in this figure, the flow topology on the train model is well represented in our LES. Beside the flow on the train, the flow patterns on the floor of the channel from LES were found to agree with the oil film visualization by Chiu and Squires [1] (see Fig. 4). Figure 4 shows that both the LES and the experimental flow contain two separations, $S_5$ and $S_6$ and one attachment line $A_3$ at the same position in the flow downstream of the train. The upstream flow in our LES was found to be attached in agreement with the experimental observations.

Although the flow was found to separate on the top of the model, the separation bubble was found to be extremely thin in the wall-normal and the streamwise direction. Besides, it was found that this bubble exists only for some times in the instantaneous flow. All this implies that its influence on the wake flow is small.

The resulting time-averaged wake flow is very complex with multiple vortices (Fig. 2). All these structures were found to be in agreement with the experimental observations. Beside the time-averaged, we have studied the instantaneous flow and found the dominant non-dimensional frequencies of the side and the lift forces at $St = 0.07$ and $St = 0.1$, respectively. These frequencies are in the interval of the resonance frequencies of a real high speed train ($0.04 < St < 1.2$) which implies possible danger of their interaction. More results from our LES of the $90^o$ yaw angle flow can be found in [5].

Here we present only our preliminary results from simulations of the $35^o$ case, as the analysis of the results is ongoing work. Fig. 6 shows the comparison of the time-

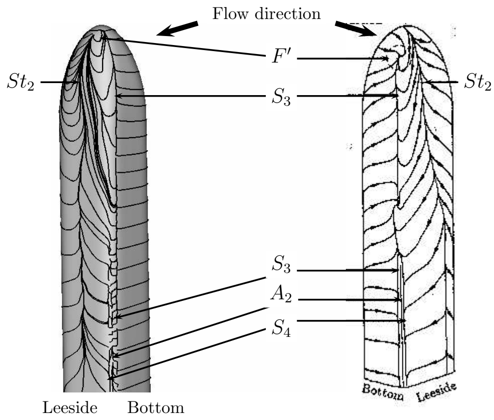


Figure 3: Surface flow pattern on the lee-side and bottom-side face. Left: LES flow pattern; right: experimental flow pattern (Taken from Ref. [1] with permission from Elsevier).

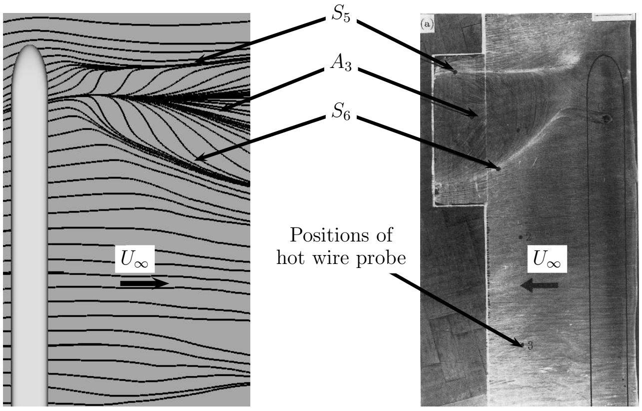


Figure 4: $90^o$ yaw angle. Ground board flow pattern. Left: LES flow pattern; right: experimental flow pattern (Taken from Ref. [1] with permission from Elsevier).

averaged flow structures in LES and experimental observations. Both the numerical and the experimental figures show similar cone-like vortices on the lee side of the train.

# 4 Lateral oscillations inside tunnels

Stability problems due to aerodynamic effects occur not only when trains are affected by cross wind but also when passing other objects such as other trains and infrastructure. Here we report our use of LES to study aerodynamically induced tail vibrations of high speed trains inside narrow double-track tunnels. These are recognized as a problem in Japan while other nation's high speed train services have not yet reported similar difficulties.

Two different trains were studied, one Japanese Shinkansen S300 train and one German ICE2 train. Despite similarities of these two trains, the problems are reported only for the former. Several calculations of trains of different lengths and with or without inter-carriage gaps are made. The shortest model that enabled us to resolve the near-wall coherent structures had a length of $6.55h$ and $7.61h$ for the ICE2 and S300 models, respectively, $h$ being the height of the train (Fig. 7). Models in other simulations were longer (around $26.2h$) and were used to check the development of the lateral oscillations along the train. The Reynolds number in all simulations was $10^5$ based on the inlet velocity and the height of the train.

Cross section of the tunnel in Japan is smaller and the body of the train is closer to the tunnel than in Germany. In order to isolate the influence of the form of the train on the lateral oscillations, we have constructed an artificial tunnel for the ICE2 train that has similar cross section compared to the tunnel used for S300. The model was located

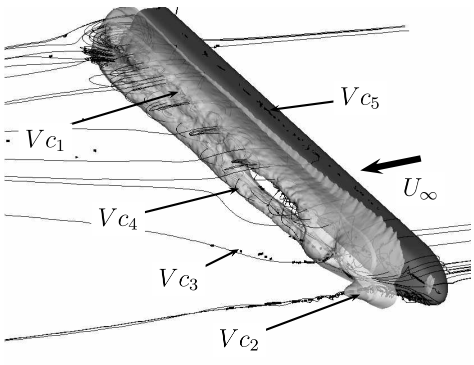


Figure 5: $90^o$ yaw angle. The isosurface of the time-averaged static pressure in the wake flow ($p = -0.2$). Streamlines are produced using vortex cores as emitters.

$8h$ from the inlet and $16h$ from the outlet of the tunnel (Fig. 7). All models except one containing artificial inter-carriage gaps (see Fig. 8c) were smooth.

### 4.1 Boundary conditions and numerical method

As the grid resolution on the body of the train was sufficient to resolve the near-wall structures in the simulation of the short train (length of $6.55h$ and $7.61h$ for the ICE2 and S300 models, respectively), no-slip boundary conditions were used on the surface of the body. Inlet velocity was prescribed to the tunnel walls. Velocity profile constant in time was used at the inlet and homogeneous Neumann boundary conditions were used at the outlet. Such an outlet boundary condition is used due to the absence of convective outlet boundary conditions in the commercial package Star-CD that was used for these simulations. Three computational grids containing 2.0, 2.5 and 6.8 million nodes were used for the short model simulations.

## 5 Results

Previous numerical studies by Suzuki [10] identified coherent structures along the train, on the side closer to the tunnel wall, that grow in size as the flow develops toward the rear end of the train. However the resolution in his simulation was modest and was far from the resolution used in our LES. In our first LES using coarse grid we have also observed structures similar to those found in [10]. We have found that these structures were small and high frequent and could not influence the ride comfort of the train. Besides, these structures became smaller when the computational grid was refined (Fig. 9a). Instead we found structures on the center side of the tunnel (Fig. 9b). These structures are too weak to cause the lateral oscillations of the train but they interact with the flow around the rear end and influence the position of separation of the flow at the rear end.

In order to find if the flow around a short train model has similar characteristics as that of the real 400 m long train, we have computed power spectral density of the side force signal. No dominant frequency was found in the ICE2 flow, while the peak at non-dimensional frequency of $St = 0.09$ was found in the S300 signal. This can be compared to $St \simeq 0.1$ recorded at full scale tests. Thus our LES of the flow around short model can produce the flow similar to that at the real-scale train at cruising velocity of around 280 km/h. Besides, these LES have shown that two trains produce different flow characteristics at similar flow conditions (similar tunnel and Reynolds number). Note that tunnels are diffrenet in reality.

Using inter-carriage gaps we found that these discontinuities can generate significant unsteady forces in the intermediate carriages. This explains the lateral vibration that take place on coaches other than that of the tail. This simulation also showed that large pressure disturbances produced by the inter-carriage gaps control the frequency of the forces at the rear end.

Simulations with the smooth models showed strong correlation between the side and lift forces for the Shinkansen model, whereas the same does not exist for the ICE2. Such a correlation of two motions (up and in the lateral direction) is likely more disadvantageous

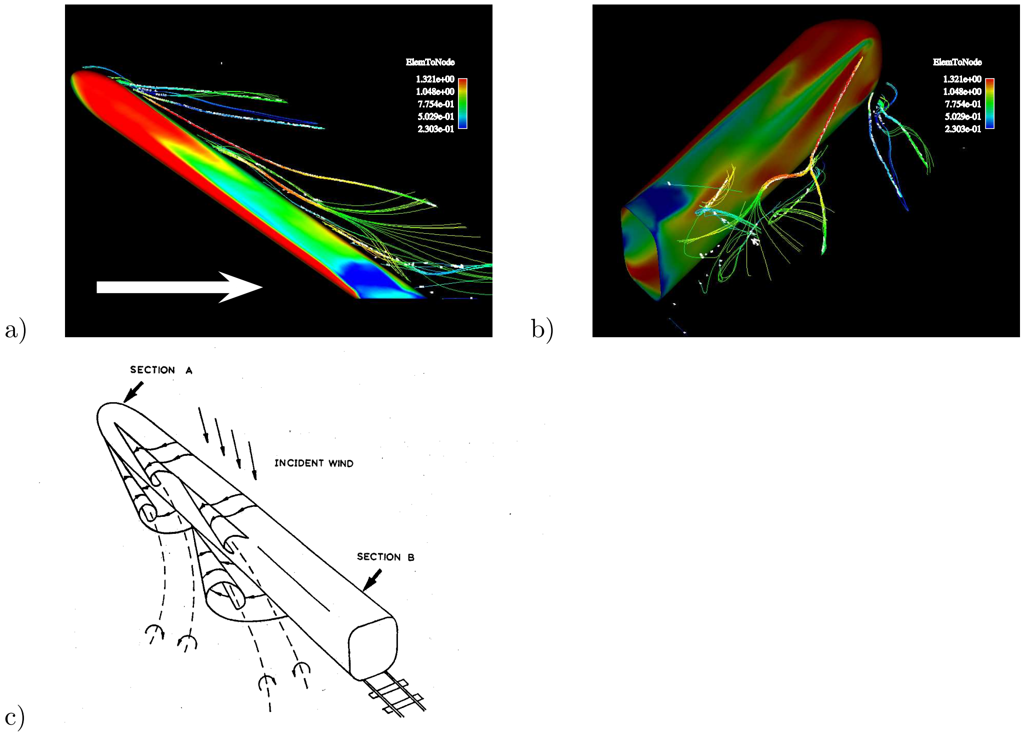


Figure 6: Flow around the train under the influence of the cross wind at an yaw angle of $35^o$. a) View from above of our LES flow. Body is colored with the surface pressure. Streamlines in the wake are produced using vortex cores as emitters. b) View from behind of our LES flow. c) Schematic representation of the flow from experimental observations by Chiu and Squires [1].

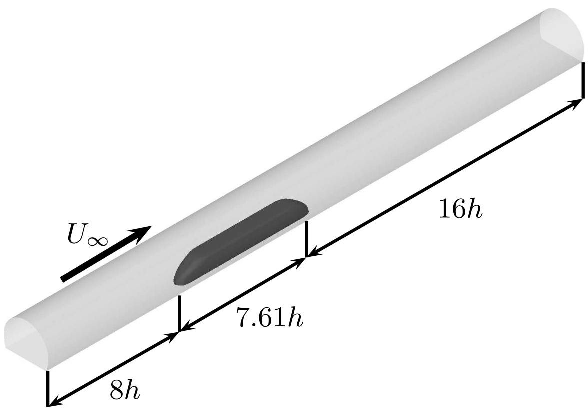


Figure 7: Computational domain of the Shinkansen model inside the tunnel. Both the tunnel and the floor are moving with the inlet velocity $U_\infty$.

for the comfort. The difference in stability between these two trains is probably due to the shape of the rear end where more curved surfaces such as those on Shinkansen model are more damaging for the stability as the position of the separation varies more than in the case of ICE2. Our LES also showed that the most of the unsteady forces of the tail coach is produced within the last $2.6h$ from the rear of the train.

From our LES we have found that the chief reasons for the tail vehicle vibrations of Shinkansen train are: high speed, wide car body in combination with the relatively large track spacing yielding small wall clearance inside the narrow tunnels, more rounded tail compared to that of ICE2 and discontinuities in the trains profile (such as inter-carriage gaps and boogies). More details on our simulation of the train flow in tunnel can be found in [2, 3, 4].

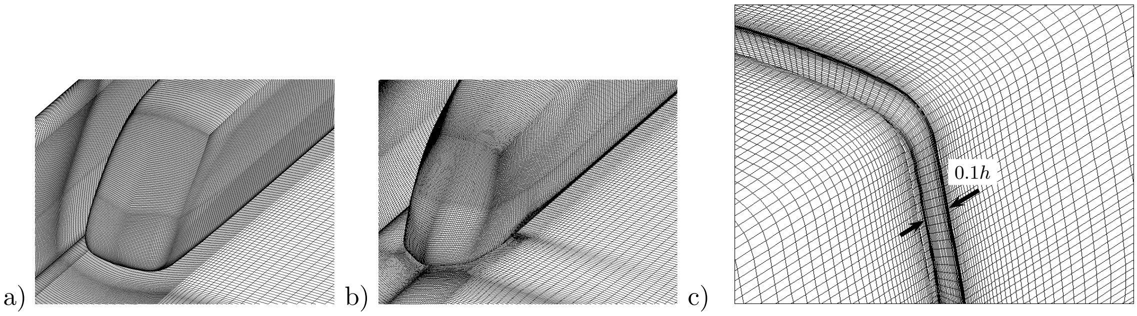


Figure 8: Computational grid on the surface of a)ICE2; b) Shinkansen train and c) artificial inter-carriage gaps of Shinkansen train.

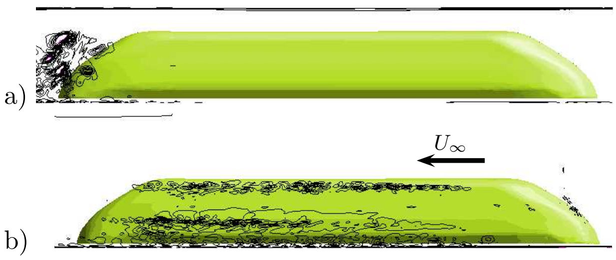


Figure 9: LES of the short Shinkansen model using 6.8 million nodes. Isolines of the streamwise vorticity component $\omega_x$. View from a) tunnel wall; b) center of the tunnel.

# 6 Conclusions

In the present paper we have demonstrated use of large eddy simulation for prediction of two flows around high speed trains; that of the flow under the influence of cross-wind and that of the flow around trains passing narrow double-track tunnel. In both cases the train is subject to unsteady forces. Study of such flow phenomena requires method of analysis that can provide us with accurate information on time-dependent flow. LES is inherently time-dependent and if properly applied it can provide us with deeper understanding of flow mechanisms responsible for variation of aerodynamic forces. Unfortunately, LES of flow around high-speed train at operating Reynolds number is prevented today by insufficient computer resources. However the target of our study in the present work was flow at lower Reynolds number that still contains the chief characteristics of the original high Reynolds number flow. Similar is already used in experimental studies and numerical studies of flows around road vehicles [6, 7, 8, 9].

LES predicted flows in agreement with low Reynolds number experimental simulations in both cases but also flow phenomena (such as frequency of the lateral oscillation of the train in narrow tunnel) observed at the higher operating Reynolds number. The advantage of LES compared with the experimental studies is that the flow can be *recorded* in time in the entire computational domain and used *a posteriori* for understanding of flow. For example, visualizing of instantaneous flow in the tunnel flow has enabled us to find the interaction of the small-scale longitudinal vortices along the train on the center side of the tunnel with the wake structures.

Beside the aerodynamic phenomena studied in the present paper, there are several other problems which solution require use of time-dependent numerical simulations. One example is uprise of ballast under and behind the train as a result of aerodynamic effects at high velocity of the train. These are caused by the suction effects under the train and the slipstream effect behind the train. Another phenomena that requires time-dependent simulation is noise generated by the interaction of the flow with the train body, i.e., aeroacoustic. In the present work we have studied the influence of the steady cross-wind on the train. However the more dangerous for the security is when the high-speed train is affected by wind gusts. Beside the unsteadiness caused by the nature of turbulent flow, such flow contains the unsteadiness generated by the boundary conditions, namely wind gust. This is also a flow that can easily be studied by LES. The influence of a wind gust is relatively short which implies that simulation time should not need to be very long making LES an excellent tool for study of such a flow. Note that the most of the computational effort in LES is due to the long averaging time required to obtain statistics of low-frequency motions.

# 7 Acknowledgments

The research about cross-wind stability of high-speed trains is financed by the Swedish Agency for Innovation System (VINNOVA) and supported by Bombardier Transportation and Scania. Computer time for these simulations on NSC (National Supercomputer Center in Sweden), SWEGRID and UNICC at Chalmers are gratefully acknowledged.

Simulations of the flow around high-speed train in tunnels is financed by Banverket (Swedish National Rail Administration) under contract No. S02/850/AL50. Bombardier Transportation Sweden AB has contributed with computer resources.

# References

[1] T. W. Chiu and L. C. Squire. An experimental study of the flow over a train in a crosswind at large yaw angles up to $90^o$. *Journal of Wind Engineering and Industrial Aerodynamics*, 45:47–74, 1992.

[2] B. Diedrichs, M. Berg, and S. Krajnović. Large eddy simulations of a typical european high-speed train inside tunnels. In *SAE 2004 World Congress*, SAE Paper 2004-01-0229, Detroit, Michigan, USA, 2004.

[3] B. Diedrichs, M. Berg, and S. Krajnović. Large Eddy Simulations of the Flow Around High-Speed Trains Cruising Inside Tunnels. In *ECCOMAS 2004, P. Neittaanmaki, T. Rossi, S. Korotov, E. Onate, J. Periaux, and D. Knorzer (eds.)*, July 25-28 2004, Finland, 2004.

[4] B. Diedrichs, S. Krajnović, and M. Berg. On Tail Vibrations of Very High-Speed Trains Cruising Inside Tunnels, (submitted for publication). *Journal of Wind Engineering and Industrial Aerodynamics*, 2005.

[5] H. Hemida, S. Krajnović, and L. Davidson. Large eddy simulations of the flow around a simplified high speed train under the influence of cross-wind. In *17th AIAA Computational Dynamics Conference*, Toronto, Ontario, Canada, 2005.

[6] S. Krajnović and L. Davidson. Numerical Study of the Flow Around the Bus-Shaped Body. *ASME: Journal of Fluids Engineering*, 125:500–509, 2003.

[7] S. Krajnović and L. Davidson. Flow Around a Simplified Car, Part I: Large Eddy Simulation, september 2005. *ASME: Journal of Fluids Engineering*, 127, 2005.

[8] S. Krajnović and L. Davidson. Flow Around a Simplified Car, Part II: Understanding the Flow, september 2005. *ASME: Journal of Fluids Engineering*, 127, 2005.

[9] S. Krajnović and L. Davidson. Influence of floor motions in wind tunnels on the aerodynamics of road vehicles, (in press). *Journal of Wind Engineering and Industrial Aerodynamics*, 2005.

[10] M. Suzuki. Flow-induced vibrations of high-speed trains in tunnels. In *Lecure Notes in Applied Mechanics*, 2002.